

Observation of the spontaneous vortex phase in the weakly ferromagnetic superconductor $\text{ErNi}_2\text{B}_2\text{C}$: A penetration depth study

Elbert E. M. Chia and M. B. Salamon

Department of Physics, University of Illinois at Urbana-Champaign, 1110 W. Green Street, Urbana Illinois 61801

Tuson Park

Los Alamos National Laboratory, MST-10, Los Alamos, New Mexico 87545

Heon-Jung Kim and Sung-Ik Lee

National Creative Research Initiative Center for Superconductivity and Department of Physics, Pohang University of Science and Technology, Pohang 790-784, Republic of Korea

(Dated: December 2, 2024)

The coexistence of weak ferromagnetism and superconductivity in $\text{ErNi}_2\text{B}_2\text{C}$ suggests the possibility of a spontaneous vortex phase (SVP) in which vortices appear in the absence of an external field. We report evidence for the long-sought SVP from the in-plane magnetic penetration depth $\Delta\lambda(T)$ of high-quality single crystals of $\text{ErNi}_2\text{B}_2\text{C}$. In addition to expected features at the Néel temperature $T_N = 6.0$ K and weak ferromagnetic onset at $T_{WFM} = 2.3$ K, $\Delta\lambda(T)$ rises to a maximum at $T_m = 0.45$ K before dropping sharply down to ~ 0.1 K. We assign the 0.45 K-maximum to the proliferation of spontaneous vortices. A model proposed by Koshelev and Vinokur explains the increasing $\Delta\lambda(T)$ as the vortex density increases and its subsequent decrease below T_m as defect pinning suppresses vortex hopping.

PACS numbers: 74.25.Ha, 74.25.Qt, 74.70.Dd, 74.25.Nf

It is now clear that the borocarbide superconductor $\text{ErNi}_2\text{B}_2\text{C}$ develops weak ferromagnetism (WFM) below $T_{WFM} = 2.3$ K while remaining a singlet superconductor^{1,2}. The question naturally arises as to how these two seemingly incompatible orders — ferromagnetism and superconductivity, can coexist microscopically. Clearly coexistence can occur only if the internal field B generated by the ferromagnetic moment does not exceed H_c for a Type-I, or H_{c2} for a Type-II, superconductor (SC). However, for a Type-II SC, a spontaneous vortex phase (SVP) is predicted to appear if B further satisfies the condition $H_{c1} < B \sim 4\pi M < H_{c2}$ ^{3,4,5}. In this phase vortices are *spontaneously* generated, in the absence of any external field. The screening currents associated with these vortices serve to shield the superconducting regions from the intrinsic magnetization; however, the vortices are qualitatively different from those generated by externally applied fields⁶. In this Letter we provide strong evidence for the existence of the SVP from penetration depth data on a high quality single-crystal of $\text{ErNi}_2\text{B}_2\text{C}$.

There have been previous SVP reports that we consider inconclusive. Ng and Varma⁷, for example, interpreted small angle neutron scattering (SANS) data on $\text{ErNi}_2\text{B}_2\text{C}$ as a prelude to the SVP. That paper⁸ reported that the vortex-line lattice begins to tilt away from the c -axis (along which the magnetic field is applied) towards the a - b plane as the temperature is decreased through the ferromagnetic transition at T_{WFM} . However, the tilt can merely be a result of the vector sum of the applied field and the internal field produced by the ferromagnetic domains in the basal plane. Additional evidence was provided by SANS data⁹ with the applied magnetic field in

the basal plane. A large field was applied to align ferromagnetic domains. When the field was removed, the flux line lattice was found to persist below T_{WFM} but to disappear above it. However, owing to the low T_c (~ 8.5 K) and increased pinning below T_{WFM} ¹⁰, trapped flux cannot be ruled out.

Among the magnetic members of the rare-earth (RE) nickel borocarbide family, $\text{RENi}_2\text{B}_2\text{C}$ (RE = Ho, Er, Dy, etc), $\text{ErNi}_2\text{B}_2\text{C}$, is a particularly good candidate for study. Superconductivity arises at $T_c \approx 11$ K and persists when antiferromagnetic (AF) order sets in at $T_N \approx 6$ K¹¹. In the AF state the Er spins are directed along the b -axis, forming a transversely polarized, incommensurate sinusoidal spin-density-wave (SDW) state, with modulation vector $\delta = 0.553a^*$ ($a^* = 2\pi/a$)¹². The appearance of higher-order reflections at lower temperatures¹ signals the development of a square-wave modulation, with regular spin slips spaced by $20a$. Below 2.3 K WFM appears, corresponding to approximately one Er magnetic moment per twenty unit cells, clearly correlated with spin slips.

In this Letter, we report measurements of the in-plane magnetic penetration depth $\Delta\lambda(T) = \lambda(T) - \lambda(T_{base})$, in single crystals of $\text{ErNi}_2\text{B}_2\text{C}$ down to $T_{base} = 0.12$ K using a tunnel-diode based, self-inductive technique at 21 MHz. Superposed on the usual decrease in $\Delta\lambda(T)$ we observe a slight dip at the Néel temperature $T_N = 6.0$ K and a small feature at $T_{WFM} = 2.3$ K, where the weak ferromagnetic component sets in. Unexpectedly, $\Delta\lambda(T)$ increases significantly again below T_{WFM} , reaching a sharp maximum at $T_m = 0.45$ K, before decreasing sharply down to 0.12 K. We interpret the increase to the T_m -maximum as evidence for the development of the

SVP in this material. Below T_m the vortices are pinned by defects, hence they no longer contributed to an excess penetration of the rf field. We treat our data in the context of a two-level model proposed by Koshelev and Vinokur (KV)¹³, where the penetration of the applied ac magnetic field is assisted by jumps of vortex lattice regions between different metastable states (two-level systems).

According to KV, the frequency response of the vortex lattice pinned by point defects can be classified into three frequency regimes. At high frequency, absorption is caused by viscous motion of the vortex lattice as a whole and one can neglect the pinning potential. At lower frequencies the absorption is dominated by small oscillations of the pinned lattice near equilibrium (Campbell regime). At still lower frequencies, jumps of lattice regions between different metastable states (two-level systems) come into play and dominate the absorption. The last two mechanisms of absorption are sensitive to the pinning strength, which depends on the value of the magnetic field B inside the sample. At small field, vortices are pinned independent of one another. When B exceeds a characteristic value B_p , pinning becomes collective¹⁴, where the vortex lattice is split into volumes that are pinned independently, with correlation regions having length L_{c0} parallel to the field. We consider the case $H_{c1} < B, B_p \ll H_{c2}$, i.e. in the mixed state.

The two-level model, which we use to explain our data, has the pinning state characterized by a large number of metastable configurations. If we shift any volume V of the vortex lattice, then a finite probability exists that at some distance u there is another state with a similar energy. At finite temperatures such regions of the lattice jump between metastable states. Any two-level system can be characterized by four parameters: its volume V , average flux displacement u , energy barrier U and energy difference Δ between the metastable states. Under the action of an applied ac field of frequency ω , an ac screening current is formed to screen the field out of the sample. The vortices then experience an ac Lorentz force which causes them to move and jump to a nearby metastable state. The motion of the vortices, which carry magnetic fields, then causes an increase in ac field penetration into the sample, resulting in an increase in the effective penetration depth λ_{eff} . As the temperature decreases, there is insufficient thermal energy to overcome the barrier U . No jumping takes place, the vortices are frozen, and hence there is no extra penetration. One therefore recovers the London penetration depth $\lambda_{||}$ at the lowest temperatures. In the correct frequency regime the two-level response dominates over the oscillating one, and the penetration is estimated as

$$\lambda_{eff}^2(T) = \lambda_{||}^2(T) + \frac{B^2(T)n_{tl}}{16\pi T} \left\langle \frac{V^2 u^2}{(1 + (\omega\tau(T))^2) \cosh^2(\Delta/T)} \right\rangle \quad (1)$$

$\langle \dots \rangle$ denotes an average over the distribution of two level systems. Here $\lambda_{||}(T)$ is the London penetration depth

in the absence of vortices; B , the internal field; n_{tl} , the concentration of two-level systems; and τ , the jump time between metastable states. Only the subset of two-level systems for which $\omega\tau \approx 1$ contribute to λ_{eff} . In the low-field region ($B < B_p$), the vortex lines move independently, and their presence does not change the penetration depth considerably ($\lambda_{eff} \approx \lambda_{||}$). However, in the collective pinning state ($B > B_p$), the jumping volume is not too small, and the characteristic distance at which the nearest metastable state exists is approximately the radius of the pinning force $u \approx \xi_{||}$.

Details of sample growth and characterization are described in Ref. 11. The samples were then annealed according to conditions described in Ref. 15. Measurements were performed utilizing a 21-MHz tunnel diode oscillator¹⁶ with a noise level of 2 parts in 10^9 and low drift. The magnitude of the ac field was estimated to be less than 40 mOe. The cryostat was surrounded by a bilayer Mumetal shield that reduced the dc field to less than 1 mOe. The very small values of the ac and dc field in our system ensure that our measurement is essentially a zero-field one, thereby eliminating the possibility of trapped flux. The sample was mounted, using a small amount of GE varnish, on a single crystal sapphire rod. The other end of the rod was thermally connected to the mixing chamber of an Oxford Kelvinox 25 dilution refrigerator. The sample temperature is monitored using a calibrated RuO₂ resistor at low temperatures ($T_{base} - 1.8$ K), and a calibrated Cernox thermometer at higher temperatures (1.3 K – 12 K).

The deviation $\Delta\lambda(T) = \lambda(T) - \lambda(0.12 \text{ K})$ is proportional to the change in resonant frequency $\Delta f(T)$ of the oscillator, with the proportionality factor G dependent on sample and coil geometries. We determine G for a pure Al single crystal by fitting the Al data to extreme nonlocal expressions and then adjust for relative sample dimensions¹⁷. Testing this approach on a single crystal of Pb, we found good agreement with conventional BCS expressions. The value of G obtained this way has an uncertainty of $\pm 10\%$ because our sample, with approximate dimensions $1.2 \times 0.9 \times 0.4 \text{ mm}^3$, has a rectangular, rather than square, basal area¹⁸.

Figure(1) shows the temperature-dependence of the in-plane penetration depth $\Delta\lambda(T)$. We see the following features: (1) onset of superconductivity at $T_c^* = 11.3$ K, (2) a slight dip at $T_N = 6.0$ K, (3) a peak at $T_{WFM} = 2.3$ K, (4) another sharp peak at $T_m = 0.45$ K, and (5) an eventual downturn below T_m . The features at T_N and T_{WFM} have not been seen in previous microwave measurements of $\Delta\lambda(T)$ on either thin-film¹⁹ or single-crystal ErNi₂B₂C²⁰; the T_N -feature has been observed in SANS data²¹. The large value of T_c and the resolvability of the features at T_N and T_{WFM} attest to the high purity of the samples.

Figure(2) shows the data below T_{WFM} . The solid line shows the fit of Eqn. 1 to the data below T_{WFM} . In this fit, we follow KV and replace $\langle \dots \rangle$ with values that characterize an effective number n_{tl}^{eff} of active two-

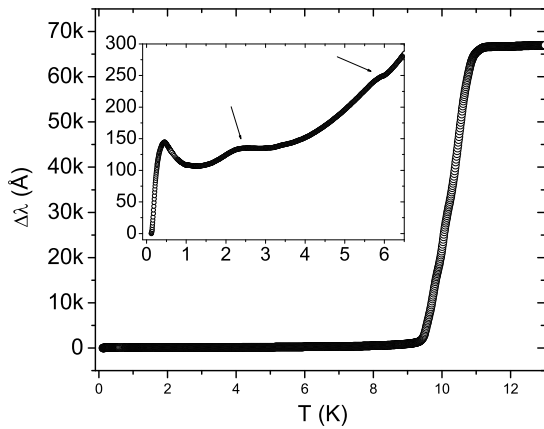


FIG. 1: Temperature dependence of the penetration depth $\Delta\lambda(T)$ from 0.12 K to 13 K. Inset shows the low-temperature region. The arrows point to the features at T_N and T_{WFM} .

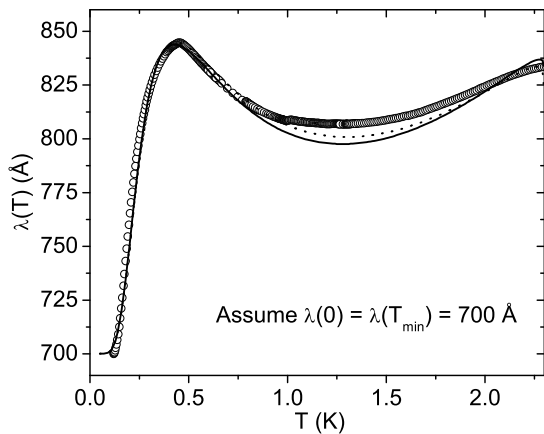


FIG. 2: (○) Temperature dependence of the penetration depth $\Delta\lambda(T)$ in the WFM phase. We've assumed $\lambda(T_{base}) \approx \lambda(0) = 700 \text{ \AA}$ from Ref. 21. The solid line is the fit of the data to Eqn. 1 for $n=0.21$, while the dotted line is that of $n=0.125$. The values of other parameters are mentioned in the text.

level systems. The values of the following quantities will be derived later: $B(T=0) \approx 1100 \text{ G}$, $u \approx \xi_{\parallel} \approx 150 \text{ \AA}$, $V = L_{c0}u^2 = 5.4 \times 10^{-16} \text{ cm}^3$, and $\tau \sim \tau_0 \exp(U_{\omega}/T)$, where $\tau_0 = 2.2 \times 10^{-9} \text{ s}$ is the jumping time prefactor. The temperature-dependence of the internal magnetic field $B(T)$ can be obtained by fitting magnetization values in Ref. 22 to the expression

$$B(T) \sim \left(1 - \frac{T}{T_{WFM}}\right)^n \quad (2)$$

giving $n=0.21$. This value of n is between the 2D-Ising value of 0.125 and the 3D-Ising value of 0.31, which is

reasonable because in $\text{ErNi}_2\text{B}_2\text{C}$ the spins lie on sheets normal to the a axis and are confined to be along or anti-along the b axis, yet there is also 3D behavior in the superconductivity. Because U_{ω} and Δ are strongly correlated, we make the reasonable assumption that all metastable states are equivalent ($\Delta = 0$) and choose the energy barrier $U_{\omega} = 0.49 \text{ K}$ and pinning density $n_{tl}^{eff} = 1.61 \times 10^{11} \text{ cm}^{-3}$ that best fit the peak in $\lambda_{eff}(T)$. This value of the barrier makes $\omega\tau \approx 1$ near 1 K. We expect $\lambda_{\parallel}(T)$ to exhibit a power-law temperature dependence at low temperatures from the combination of gap-minima observed in non-magnetic borocarbides and the increased pair-breaking as Er spins disorder. Consequently, we set $\lambda_{\parallel}(T) = \lambda_{\parallel}(0)(1 + bT^2)$ with $b = 0.036 \text{ K}^{-2}$ the third adjustable parameter in the fit. For comparison, we show the (dotted-line) fit with $n = 1/8$ (2D-Ising model) for which $U_{\omega} = 0.49 \text{ K}$, $n_{tl}^{eff} = 1.57 \times 10^{11} \text{ cm}^{-3}$, and $b = 0.033 \text{ K}^{-2}$. Both fits reproduced the qualitative features of the data, though the latter curve fits the data slightly better.

To justify our application of the two-level model to our data, we must evaluate various physical parameters in the model. We start with the measured quantities: zero-temperature in-plane penetration depth $\lambda_{\parallel}(0) \approx 700 \text{ \AA}$ and coherence length $\xi_{\parallel} \approx 150 \text{ \AA}$ (and $\kappa = \lambda_{\parallel}(0)/\xi_{\parallel} = 4.7$) from Ref. 21, ferromagnetic moment $M \approx 0.62\mu_B/\text{Er} \approx 100 \text{ Oe}$ well below T_{WFM} from Ref. 10, and the normal-state resistivity $\rho_n(T_c^*) = 5.8 \mu\Omega \text{ cm}$ that we measured for our sample. The value of M corresponds to an internal field $B \sim 4\pi M = 1100 \text{ G}$, which is greater than $H_{c1} \sim 500 \text{ G}$, putting us in the mixed state. From these values we can calculate the following quantities: (1) depairing current density $j_s = c\Phi_0/(12\sqrt{3}\pi^2\xi_{\parallel}\lambda_{\parallel}^2) \approx 1.5 \times 10^8 \text{ A/cm}^2$, (2) critical current density $j_c = 4cM_h/L = 1.9 \times 10^4 \text{ A/cm}^2$ from the Bean model²³, where $L \approx 1 \text{ mm}$ is the length of the sample¹⁰, (3) viscous drag coefficient $\eta \approx \Phi_0^2/(2\pi\xi_{\parallel}^2\rho_n c^2) = 5.6 \times 10^{-7} \text{ erg s cm}^{-3}$ from the Bardeen-Stephens model. Note that M_h is the magnetization obtained in a hysteresis measurement¹⁰, and is distinct from the ferromagnetic moment M . As usual $\Phi_0 = 2.07 \times 10^{-7} \text{ G cm}^2$ is the flux quantum. From j_s and j_c we obtain $L_{c0} = 2.4 \mu\text{m}$ by solving the transcendental equation

$$x^2 = \frac{j_s}{j_c} \ln x, \quad (3)$$

where $x \equiv \gamma L_{c0}/\xi_{\parallel}$ and $\gamma = \lambda_{\perp}/\lambda_{\parallel} \approx 1.3^{11}$. The jumping time prefactor can be calculated from $\tau_0 = \eta\xi_{\parallel}c/(\Phi_0 j_c)$ to get $\tau_0 = 2.2 \times 10^{-9} \text{ s}$.

Next we determine whether our material is in the individual or collective pinning regime, by calculating B_p . It is given by¹³

$$B_p = \frac{\Phi_0(\ln x)^{4/3}}{L_{c0}^2}, \quad (4)$$

from which we obtain $B_p \approx 20 \text{ G}$. We are therefore in the collective pinning regime ($B \approx 4\pi M > B_p$). The

characteristic value of the energy barrier for flux flow is given by

$$E_p \sim (B/c)j_c\xi_{\parallel}V. \quad (5)$$

Near H_{c1} , the vortex lattice parameter $\sqrt{\Phi_0/B} \approx \lambda$, so Eqn. 5 becomes

$$E_p \sim \frac{\Phi_0 j_c L_{c0} \xi_{\parallel}}{\kappa^2 c}, \quad (6)$$

giving $E_p = 46$ K, which is an order of magnitude larger than the temperature range of the SVP. This justifies the notion of metastable states in this material²⁴.

We can also calculate the root-mean-square (rms) diffusion amplitude of the vortex lattice, given by²⁵

$$U_{rms}(t, T) = \left[T \left(\frac{t}{\epsilon_l \eta} \right)^{1/2} \right]^{1/2}, \quad (7)$$

where t is the time of diffusion, $\epsilon_l = \Phi_0 \ln(\kappa)/(4\pi\lambda_{\parallel})^2$ is the vortex line tension, and compare this with the rms Campbell oscillation amplitude u_{rms} ²⁵

$$u_{rms}(T) = \left(\frac{TL_{c0}}{\epsilon_l} \right)^{1/2}, \quad (8)$$

if the vortex lattice were to be in the Campbell regime. We obtain $U_{rms}(2\pi/\omega, 2\text{ K}) = 17 \text{ \AA} > 9 \text{ \AA} = u_{rms}(2\text{ K})$. In fact $U_{rms} > u_{rms}$ over the entire temperature range of interest. This shows that our sample is marginally in the two-level regime. Finally, we can estimate the crossover frequency from the two-level to the Campbell regime

$$\omega_{cr} \approx (T/E_p)/\tau_0, \quad (9)$$

which gives $f_{cr} \approx 3$ MHz at $T = 2$ K. This, combined with the values of u_{rms} and U_{rms} , put us near the boundary between the two-level and Campbell regimes. Moreover, KV¹³ pointed out that the two-level absorption dominates not only at $\omega \lesssim 1/\tau$, but also in some region

$\omega > 1/\tau$. So it is still justifiable to use the two-level model to explain our data. When we applied the ac field along the basal plane, the features were qualitatively similar to the present data, including the strength and position of the features at T_N , T_{WFM} and T_m . Based on these values, we estimate the maximum density of two-level volumes to be $\sim 2.4 \times 10^{13} \text{ cm}^{-3}$ at the lowest temperatures, indicating that approximately 1% are active in our frequency window.

In conclusion, penetration depth data of single-crystal $\text{ErNi}_2\text{B}_2\text{C}$ down to ~ 0.1 K provide strong evidence for the existence of a spontaneous vortex phase below T_{WFM} . The high quality of our sample enables us to see features at T_N and T_{WFM} that have not been observed in previous studies of the penetration depth^{19,20}. We analyze this SVP data using the two-level model proposed by Koshelev and Vinokur for conventional vortices, where the absorption of the applied ac magnetic field is dominated by jumps of vortex lattice regions between different metastable states. It has been pointed out⁶, however, that the SVP lattice is much softer than a conventional lattice, and therefore especially sensitive to quenched disorder, leading us to question the extent to which parameters of the SVP lattice are similar to those of ordinary vortices. We hope the data described here will stimulate further work on the electrodynamic properties of the SVP.

This material is based upon work supported by the U.S. Department of Energy, Division of Materials Sciences under Award No. DEFG02-91ER45439, through the Frederick Seitz Materials Research Laboratory at the University of Illinois at Urbana-Champaign. Research for this publication was carried out in the Center for Microanalysis of Materials, University of Illinois at Urbana-Champaign. This work in Korea was supported by the Ministry of Science and Technology of Korea through the Creative Research Initiative Program.

¹ S.-M. Choi *et al.*, Phys. Rev. Lett. **87**, 107001 (2001).

² P. C. Canfield, S. L. Bud'ko, and B. K. Cho, Physica C **262**, 249 (1996).

³ E. I. Blount and C. M. Varma, Phys. Rev. Lett. **42**, 1079 (1979).

⁴ M. Tachiki, A. Kotani, H. Matsumoto, and H. Umezawa, Solid State Commun. **31**, 927 (1979).

⁵ H. S. Greenside, E. I. Blount, and C. M. Varma, Phys. Rev. Lett. **46**, 49 (1981).

⁶ L. Radzihovsky, A. M. Ettouhami, K. Saunders, and J. Toner, Phys. Rev. Lett. **87**, 027001 (2001).

⁷ T. K. Ng and C. M. Varma, Phys. Rev. Lett. **78**, 330 (1997).

⁸ U. Yaron *et al.*, Nature (London) **382**, 236 (1996).

⁹ H. Kawano-Furukawa, E. Habuta, T. Nagata, M. Nagao,

H. Yoshizawa, N. Furukawa, H. Takeya, and K. Kadowaki, cond-mat/0106273 (revised 1/2004).

¹⁰ P. L. Gammel *et al.*, Phys. Rev. Lett. **84**, 2497 (2000).

¹¹ B. K. Cho *et al.*, Phys. Rev. B **52**, 3684 (1995).

¹² J. Zarestky *et al.*, Phys. Rev. B **51**, R678 (1995).

¹³ A. E. Koshelev and V. M. Vinokur, Physica C **173**, 465 (1991).

¹⁴ A. I. Larkin and Y. N. Ovchinnikov, J. Low Temp. Phys. **34**, 409 (1979).

¹⁵ X. Y. Miao, S. L. Bud'ko, and P. C. Canfield, J. Alloys. Comp. **338**, 13 (2002).

¹⁶ I. Bonalde *et al.*, Phys. Rev. Lett. **85**, 4775 (2000).

¹⁷ E. E. M. Chia *et al.*, Phys. Rev. B **67**, 014527 (2003).

¹⁸ R. Prozorov, R. W. Giannetta, A. Carrington, and F. M. Araujo-Moreira, Phys. Rev. B **62**, 115 (2000).

- ¹⁹ A. Andreone *et al.*, *Physica C* **319**, 141 (1999).
- ²⁰ T. Jacobs *et al.*, *Phys. Rev. B* **52**, R7022 (1995).
- ²¹ P. L. Gammel *et al.*, *Phys. Rev. Lett.* **82**, 1756 (1999).
- ²² J. Jensen, *Phys. Rev. B* **65**, 140514(R) (2002).
- ²³ C. P. Bean, *Rev. Mod. Phys.* **36**, 31 (1964).
- ²⁴ L. B. Ioffe and V. M. Vinokur, *J. Phys. C: Solid State Phys.* **20**, 6149 (1987).
- ²⁵ G. Blatter *et al.*, *Rev. Mod. Phys.* **66**, 1125 (1994).